Available online at www.sciencedirect.com
SCIENCE DIRECT
Journal of Organometallic Chemistry 691 (2006) 1535–1543
Journal of Organometallic Chemistry
www.elsevier.com/locate/jorganchem

Trans–cis octahedral interconversion pathway in diorganotin compounds

Miriam Rossi [a], Francesco Caruso [b,*]

[a] *Vassar College, Department of Chemistry, Poughkeepsie NY 12604-0484, USA*
[b] *Istituto di Chimica Biomolecolare, Consiglio Nazionale delle Ricerche (CNR), Piazzale Aldo Moro 5, 00185 Rome, Italy*

Received 6 December 2005; accepted 7 December 2005
Available online 19 January 2006

Abstract

Using structural data from bis(bidentate)diorganotin compounds in the Cambridge Structural Database a potential pathway for *trans–cis* interconversion is envisaged with nondissociative Sn-donor bonds and retaining metal coordination number 6. C–Sn–C bond angles in the range 180–145° correspond to skewed trapezoid bipyramidal geometry for 6- and 5-membered O,O′ chelates; geometries that resemble the transition state of the *trans–cis* pathway starts forming at about C–Sn–C 134°. *cis*-Diorganotins explored in this work have C–Sn–C bond angles in the range 102–110°; it is the statistically favored configuration for diphenyltins. The proposed *trans–cis* conversion pathway is deduced from a series of geometries associated with decreasing the C–Sn–C bond angle and shows 2 weakly (secondary) bound chelating atoms lengthening their bonds until near the transition state and later strengthening; they end up *cis* to each other and opposite to the organic groups. Conversely, the other 2 (primary) donors shorten their bonds until the transition state is reached and later lengthen; they end up *trans* to each other. The entire transformation from *trans* to *cis* configuration occurs with relative rotation of 3 bonds.

Keywords: Diorganotin; *Cis–trans*; Conversion; Bidentate; Octahedron

1. Introduction

Despite ongoing efforts to clarify *trans–cis* isomerism in octahedral compounds of several metal centers, an exhaustive understanding of this process has not been possible. Notwithstanding the impressive improvements of NMR and contributions from other techniques including IR and Mössbauer spectroscopies, there is limited structural information in the solution state. In the literature several mechanistic rearrangements have been suggested to explain *trans–cis* interconversion [1–5]. Also, an interesting aspect of this isomerism is its occasional dependence on the particular choice of solvent. For instance, $PtCl_2(NH_3)_2(OH)_2$ has 3 structural *cis–trans* isomers that have been characterized with IR and X-ray diffraction. Recrystallization of one of these forms yields a 2nd one in water, but not in H_2O_2 [6]. The related $[Pt(NH_3)_4(OH)(SO_4)]^+$ *trans* isomer is converted to the *cis* one when NaOH (pH 12–13) is added [7]. Using dry chloroform as a solvent, *trans*-$Ru(CN)_2(CN\text{-}^tBu)_4$ crystallizes within days, whereas the *cis* complex precipitates after months. Using neat chloroform leads to formation of *cis* crystals only, whereas acetone yields only *trans* isomers [8].

Other factors also influence *cis–trans* geometry. For example, in $TiCl_4L_2$ octahedral complexes *cis–trans* isomerization is strongly affected by peripheral substitution of the pyrazole derivatives L [9]. *Trans*-[$RhCl_3$(DMSO-S)$_2$(DMSO-O)] isomerizes to the *cis* isomer in DMSO solution; the reverse *cis–trans* isomerization is promoted by visible light [10]. Dichloro-bis(*p*-chlorophenyl)-(4,4′-dimethyl-2,2′-bipyridyl-*N*,*N*′)-tin(IV) is synthesized as the *cis* isomer only but upon recrystallization from MeOH it

* Corresponding author. Tel.: +39 06 49913632; fax: +39 06 49913628.
E-mail addresses: francesco.caruso@icb.cnr.it, caruso@vassar.edu (F. Caruso).

0022-328X/$ - see front matter © 2005 Elsevier B.V. All rights reserved.
doi:10.1016/j.jorganchem.2005.12.021

converts to the *trans* one; in turn, the *trans* species reconverts to the *cis* one in toluene [11]. *cis–trans* interconversion on $SnL_2(monodentate)_2$ diorganotins, where L is a C···N chelating ligand, was studied in solution using NMR; processes of a different nature were responsible for this isomerization, some of them related to intramolecular Sn–N interactions [12].

Using Sn Mössbauer and IR spectroscopies and X-ray diffraction, very interesting studies on diorganotins containing halide or pseudohalide ligands were described [13,14]. The important role of solvents in stabilizing *cis* and *trans* forms was studied and *cis* isomers were found exclusively having aromatic groups. However, the octahedral *cis–trans* isomerization process is very complex since when halide or pseudohalides are missing *cis* dialkylorganotins also exist [15]. Octahedral tin has a peculiar advantage in comparison to transition elements, namely, it can expand its coordination sphere to accommodate more than 6 pairs of electrons; as a result, it can avoid breaking bonds under *trans–cis* rearrangements. Due to their natural stability, geometries that could represent intermediates in this pathway can be "frozen" and isolated in the crystalline state allowing complete structural determination. In particular, when structural features are considered, 6-coordinate diorganotin compounds show the most varied octahedral deformation. The system was analyzed theoretically by Keppert who defined this distortion as skewed trapezoidal bipyramidal (STB) [16]. Its geometry is shown in Fig. 1 for bis(bidentate)diorganotin compounds with the 2 bidentate (Qp···Qs) ligands in the equatorial plane and the 2 organic groups *trans* displayed; the Qp donor forms a covalent Sn–Q(primary) bond whereas Qs establishes a Sn–Qs(secondary) coordinative bond, that is generally longer. Therefore, when a regular octahedron becomes distorted its equatorial plane transforms to a trapezoid having the Qp···Qp′ separation as the short side and Qs···Qs′ as the longer one.

Diorganotins exist in *cis* configuration as well and the same compound can even exist in either *cis* or *trans* forms in the solid, for instance, bis(*N*-acetylhydroxylamino)dimethyltin(IV) crystallizes as the *cis* form (C–Sn–C bond angle 109.1(4)°), but as a hydrate it becomes the *trans* (C–Sn–C bond angle 157.1°) [15]. We are interested in this *trans–cis* interconversion pathway and how Q ligands can influence it. For instance, a slight modification of the *N*-acetylhydroxylamino ligand [15], *N*-methyl-*N*-acetylhydroxylamino, stabilizes a C–Sn–C bond angle of 145.8(3)° [17]. Therefore, in considering the *trans* form [15] this additional methyl substituent moves it towards the *cis* form and provides an instantaneous "frozen" view of the *trans–cis* process.

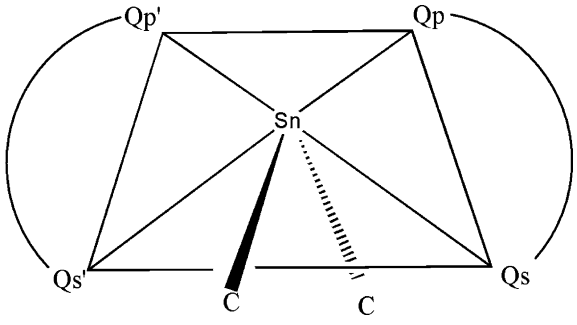

Fig. 1. Skewed trapezoidal bipyramidal arrangement in"SnQ_4C_2" diorganotins.

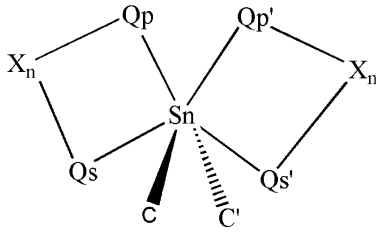

Fig. 2. Skewed trapezoidal bipyramidal configuration of bis(chelate)diorganotins "SnQ_4C_2" Q = O, N, S, etc. Qp makes a Sn–Q(primary) bond and Qs a Sn–Q(secondary) bond, Sn–Qp ⩽ Sn–Qs, Qp–Sn–Qp′ ⩽ Qs–Sn–Qs′ bond angle.

In this paper we analyze relevant compounds from the Cambridge Structural Database (CSD) to study the *trans–cis* interconversion pathway. The large number of compounds stored in the CSD allows for a statistical analysis of geometrical features related to this system. Along this path, the starting *trans* centrosymmetrical octahedral species (C–Sn–C bond angle equal 180°) will become more and more distorted and approach compounds having *cis* configuration (C–Sn–C bond angle about 90°). Bis(chelate)diorganotins, as shown in Fig. 2, are a useful set of compounds to analyze having C–Sn–C bond angle variation of about 90°. This interconversion involves only rotational modifications of the octahedral geometry, e.g., there are nondissociative Sn-donor features and the coordination number remains as 6.

2. Results and discussion

In our initial exploration of the CSD database we imposed at least one cyclic ligand and 415 hits were obtained. Compounds having monodentate ligands were excluded as they do not conserve symmetric features which help in understanding the path. Moreover, their transformation can be more complex than the one we are describing as they can even fold the C groups the opposite way, namely, toward the Qp–Sn–Qp′ angle. Another restriction we applied was to exclude compounds having links between both chelating ligands and those having the moiety Sn_2O_2 to avoid excessive rigidity. The coordination sphere of compounds in this final group (196 hits) has approximate mirror symmetry related to the SnC_2 plane; however, compounds that have one Q ligand flipped in Fig. 1 (approximately centrosymmetric species) are included. We found that the statistically relevant n range (see Fig. 2) is 1–3.

Fig. 3 shows a plot of diorganotins in the range of variation 120° ⩽ C–Sn–C bond angles ⩽ 180°; smaller values will be analyzed later.

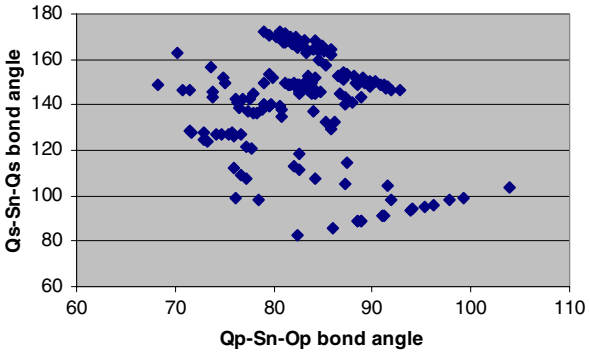

Fig. 3. Structural data of bis(chelate)diorganotins.

Several groups can be distinguished, for instance, at the bottom a linear set of points starting at [83°,83°] and ending at [105°,105°]; these belong to centrosymmetric compounds having equal Qp–Sn–Qp′ and Qs–Sn–Qs′ angles. These angles will be generally larger for 4-membered ring species than for 6-membered ones. From Fig. 3, we select specific families of compounds and analyze their structural features.

Fig. 4 depicts only bis(cyclohexa,O,O′)diorganotins, which correspond to the structure having $n = 4$ in Fig. 2. The STB trend of increasing Os–Sn–Os′ bond angles associated with decreasing Op–Sn–Op′ ones is clearly seen. Point [88°,115°] (•) [18] has refcode LIWKUX in the CSD and is anomalous; it will be discussed later when analyzing bond distances. Some points at the bottom define a straight line belonging to centrosymmetrical compounds; its range (88–98°) is probably associated with different chelate planarity.

In Fig. 5 we plot angles Op–Sn–Op′ vs C–Sn–C showing that larger Op–Sn–Op′ are associated with larger C–Sn–C bond angles as expected for STB configuration; compound LIWKUX is marked again (•).

Fig. 6 also includes compounds bis(benzoyl(thiobenzoyl)methanato-O,S)-dimethyl-tin(IV) (refcode CAYYOQ01) [19], dimethyl-(monothioacetylacetonato-O,S)-tin(IV) (refcode FUNRUB) [19] and dimethyl-bis(2-(diphenylphosphinoyl)-6-trimethylsilylphenylthiolato)-tin(IV) (refcode XARJAB) [20] (•) that contain S ligands: they follow the same trend of equivalent O ligands but are shifted towards smaller C–Sn–C values, demonstrating that

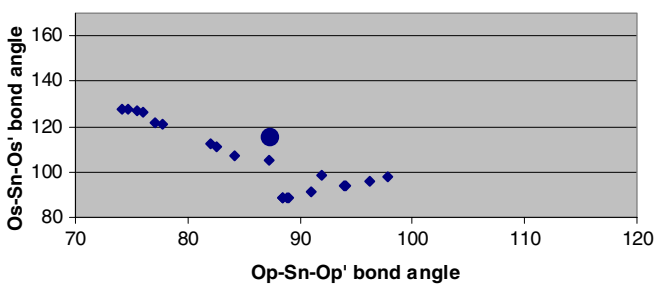

Fig. 4. Structural data of bis(cyclohexa,O,O′)diorganotins.

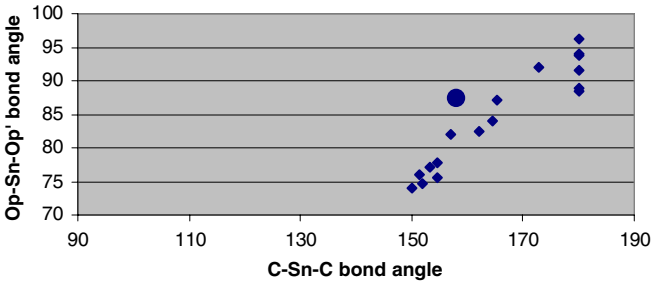

Fig. 5. Structural data of bis(cyclohexa,O,O′)diorganotins.

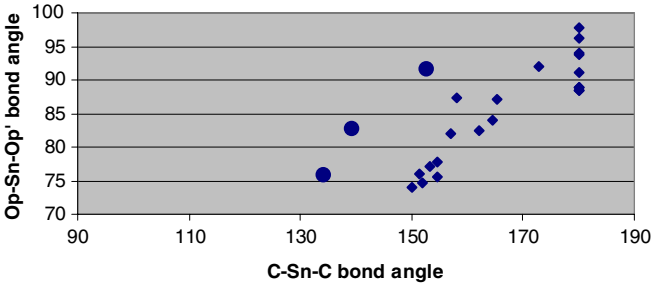

Fig. 6. Structural data of bis(cyclohexa,Q,Q′)diorganotins Q = O, S.

each specific group of ligands needs to be considered separately.

Finally, in analyzing angles Os–Sn–Os′ vs C–Sn–C we see that larger Os–Sn–Os′ are associated with smaller C–Sn–C bond angles following the STB model, see Fig. 7.

Therefore, notwithstanding the variation in planarity of the 6-membered chelate ring, bis(cyclohexa-chelate,O,O′)diorganotins follow the STB model in the experimentally observed C–Sn–C range of 150–180°.

Cyclopenta compounds ($n = 3$ in Fig. 2) show 20 hits in the CSD; they encompass a large variety of chelating atoms and there is no particular predominant set such as O,O′ for hexacyclic ones. Fig. 8 shows Os–Sn–Os′ vs Op–Sn–Op′ bond angles and the STB trend is again observed, as for related cyclohexa,O,O′ compounds above.

The STB model is also observed for Op–Sn–Op′ vs C–Sn–C angles in Fig. 9 and for Os–Sn–Os′ vs C–Sn–C bond angles in Fig. 10.

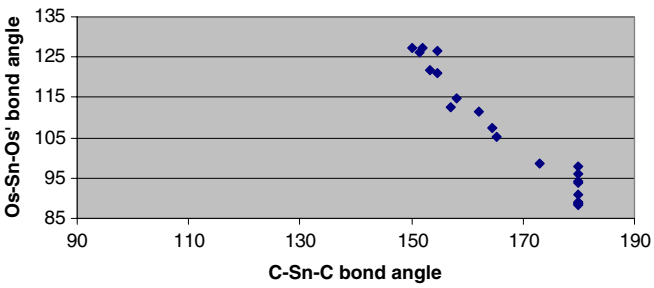

Fig. 7. Structural data of bis(cyclohexa,O,O′)diorganotins.

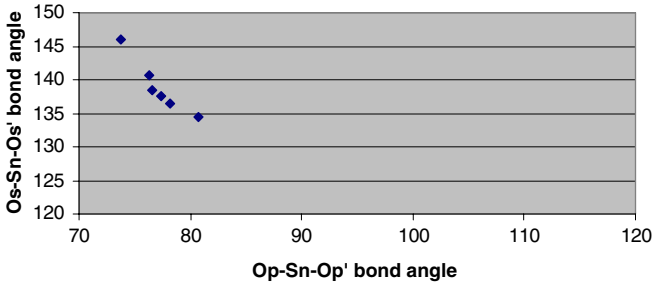

Fig. 8. Structural data of bis(cyclopenta,O,O′)diorganotins.

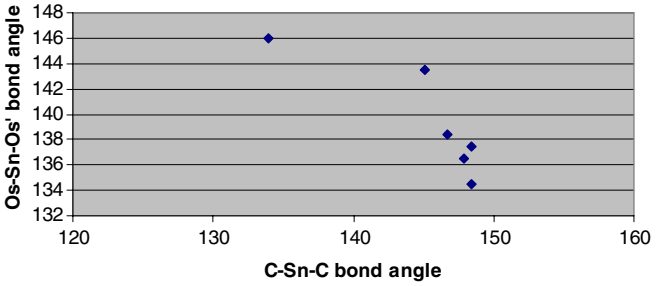

Fig. 10. Structural data of bis(cyclopenta,O,O′)diorganotins.

Compounds *trans*-bis(*N*-acetylhydroxylamino)dimethyltin(IV) · H_2O (refcode AHAMSN) [15] and *trans*-dibutylbis(tropolonato)-tin (refcode WUCQAM) [21] in this family do not follow this trend (data not shown on plot); they were excluded as a close look at their crystal packing showed them having additional ligands on the coordination sphere. For instance, *trans*-bis(*N*-acetylhydroxylamino)dimethyltin(IV) · H_2O has a weakly bound O neighbor at 2.98 Å. On the extreme left, compound bis(*n*-butyl-(*N*-phenyl-*N*-benzoylhydroxylamino))-tin (refcode WEYMUI) [22] has a C–Sn–C bond angle of 134° and appears anomalous as a wider value would be expected for its Os–Sn–Os′ value. This species shows a strong deviation of the STB model having an angle between both chelates of 10.7°. It indicates that the "transition state" between *trans* and *cis* structures in the interconversion path starts forming and it suggests its possible precursor geometry. Therefore, cyclopenta,O,O′ species extend the STB validity for the C–Sn–C angle (180–150°), shown by the cyclohexa,O,O′ compounds above, at least to 145° and suggest modifications about 135°.

Bis(cyclotetra)diorganotin compounds ($n = 2$ in Fig. 2) form the most numerous set (100 hits) as shown in Figs. 11–13.

In contrast with families seen earlier, there is only one centrosymmetric compound, whose corresponding point is isolated from the rest because these 4-membered rings stabilize structures closer to the transition state. From selected bis(cyclotetra,O,O′)diorganotins, one compound, bis(pentafluorophenylacetato)-bis(*n*-butyl)-tin (refcode RIDQAW) [23], was excluded because it has a neighboring

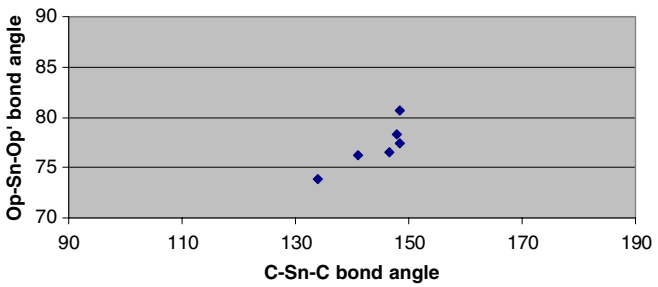

Fig. 9. Structural data of bis(cyclopenta,O,O′)diorganotins.

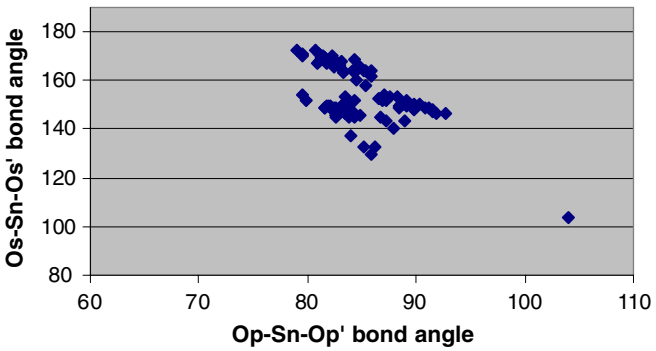

Fig. 11. Structural data of all bis(cyclotetra)diorganotins.

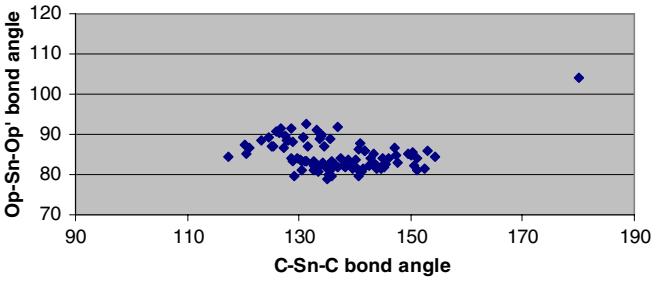

Fig. 12. Structural data of all bis(cyclotetra)diorganotins.

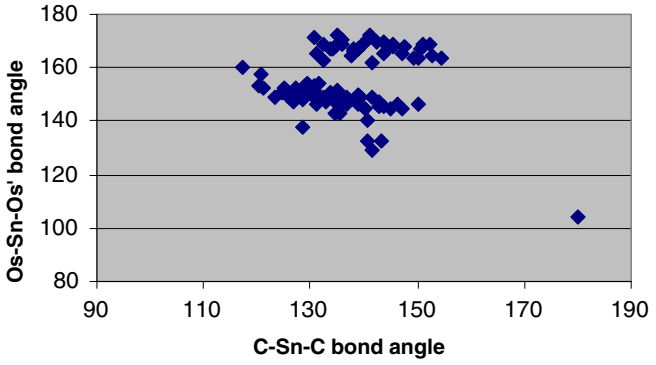

Fig. 13. Structural data of all bis(cyclotetra)diorganotins.

unit that provides 2 additional Sn–O bonds, which makes this compound 8-coordinate.

In the next plot, Fig. 14, the trend of larger Os–Sn–Os′ angles associated with smaller Op–Sn–Op′ is still seen although there is more variance.

The range of variation of Op–Sn–Op′ displayed in Fig. 15 is small, which suggests some change from related cyclohexa and cyclopenta species shown above. In addition, there are no centrosymmetric structures (C–Sn–C = 180°), probably due to the small volume that these ligands occupy in the coordination sphere. Since this family is the closest to *cis* diorganotins it can provide useful data to study the critical area of change in the *trans–cis* transformation path.

In Fig. 16, Os–Sn–Os′ vs C–Sn–C angles also show a less clear trend in comparison with cyclopenta and cyclohexa compounds, again suggesting something different than seen earlier.

Another statistically important set of cyclotetra compounds contains S ligands. However, we prefer to complete our analysis with O donors since S has a large covalent radius and consequently may induce more flexible chelate coplanar variation.

Next, all O,O′ complexes, that is, all families analyzed so far are displayed. We already saw that tetracyclo compounds show marked differences from cyclopenta and cyclohexa ones. Figs. 17 and 18 show this more clearly as the former set is well separated at the top of the next figure, whereas the latter sets are coherent and assembled at the bottom (they are displayed in Fig. 18).

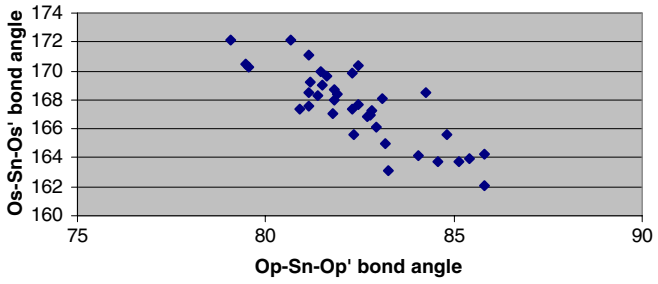

Fig. 14. Structural data of bis(cyclotetra,O,O′)diorganotins.

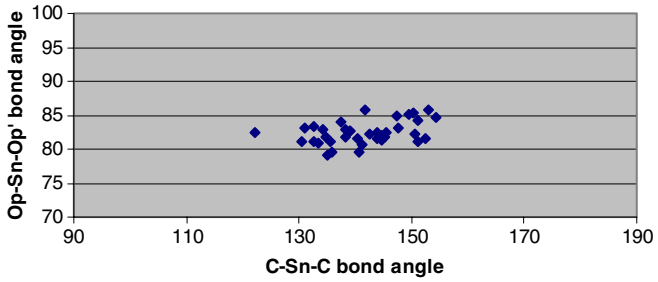

Fig. 15. Structural data of bis(cyclotetra,O,O′)diorganotins.

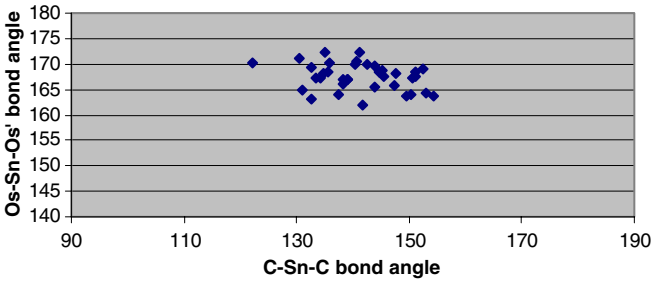

Fig. 16. Structural data of bis(cyclotetra,O,O′)diorganotins.

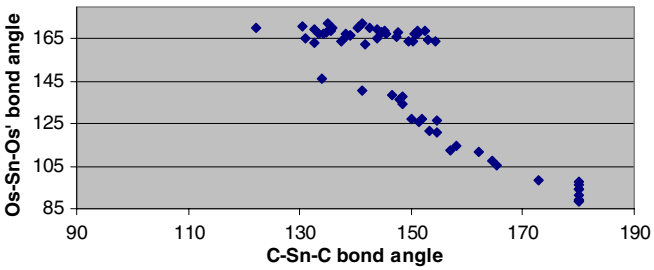

Fig. 17. Structural data of all bis(O,O′)diorganotins.

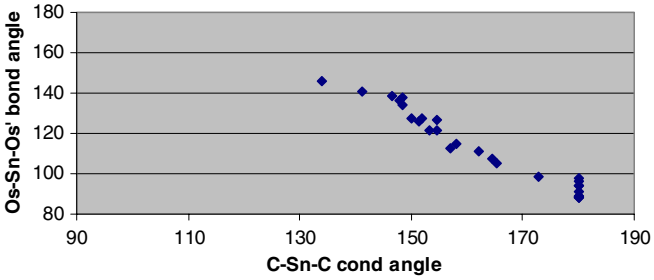

Fig. 18. Structural data of bis(cyclopenta + cyclohexa,O,O′)diorganotins.

Also, points belonging to primary bound O atoms of cyclotetra species and located at low C–Sn–C bond angles tend to be separated from cyclopenta and cyclohexa species, as seen in Figs. 19 and 20.

Geometrical features of *cis* bis(chelate)diorganotins are best analyzed using bond distances rather than bond angles, as seen below.

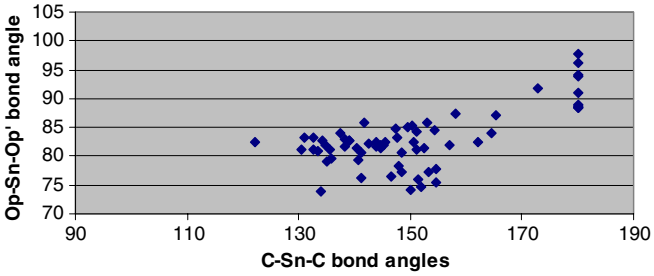

Fig. 19. Structural data of all bis(O,O′)diorganotins.

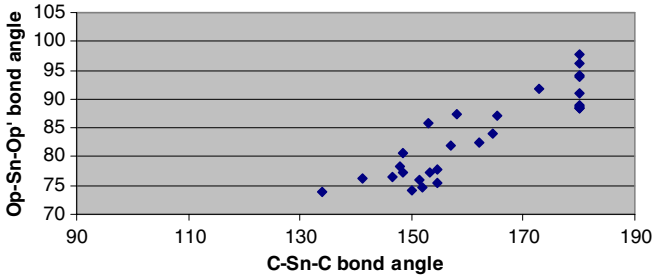

Fig. 20. Structural data of bis(cyclopenta + cyclohexa,O,O′)diorganotins.

Cis geometry is statistically favored for diphenyltins, these have C–Sn–C bonds less than 120° and can be neatly distinguished from *trans* diorganotins with larger values in Fig. 21.

Fig. 22 includes one Sn–Op and one Sn–Os bond length for non *cis* species. Note that compound with refcode LIWKUX (•) shows one Sn–Os value (2.206 Å) that is too short, however in the 2nd chelate ring Sn–Os′ bond (2.376 Å) is normal and not shown in plot.

2.1. Trans–cis interconversion

To describe the path of the donor atoms from *trans* to *cis* configurations we select bis(cyclopenta,O,N)diorganotin picolinato derivatives, the ligand is shown in Scheme 1 below; there are 7 *trans* and 6 *cis* hits in the CSD.

In Fig. 23, Sn–O bonds are shown to be shorter than Sn–N; they are equivalent to Sn–Qp and Sn–Qs, respectively in Fig. 2. Going from *trans* to *cis* structures there is

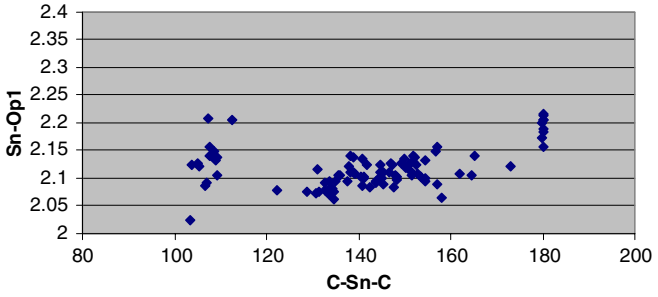

Fig. 21. Structural data of bis(cyclo,O,O′)SnC_2.

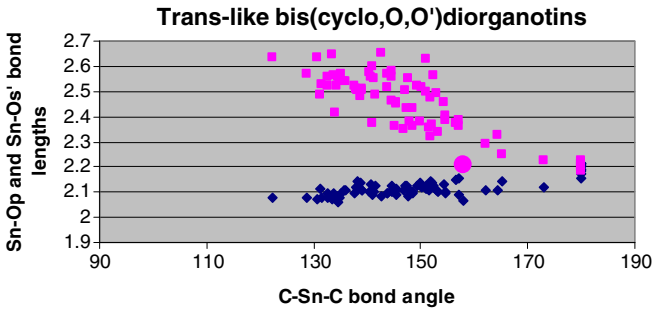

Fig. 22. Sn–Os points (square) are clearly above Sn–Op ones (diamond).

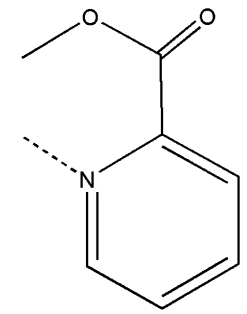

Scheme 1.

a marked decrease of Sn–N lengths and almost no variation for Sn–O.

The following Fig. 24, shows that N atoms move *cis* to each other in the *cis* structures whereas O atoms become *trans* to each other.

Figs. 25 and 26 show the structure of *trans*-di-*t*-butyl-bis(2-picolinato-N,O)-tin (refcode YORLIA) [24] with C–Sn–C bond angle of 152°, and *cis*-diphenyl-bis(2-picolinato)-tin (refcode HATKOC) [25] with C–Sn–C bond angle of 102.5°.

The resulting *trans–cis* pathway is shown in Fig. 27.

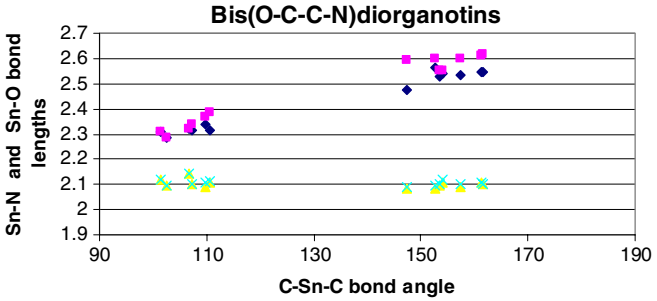

Fig. 23. Sn–N bond lengths (square and diamond), equivalent to Sn–Qs and Sn–Qs′ in Fig. 2, are long; Sn–O ones (cross and triangle), equivalent to Sn–Qp and Sn–Qp′ in Fig. 2, are shorter.

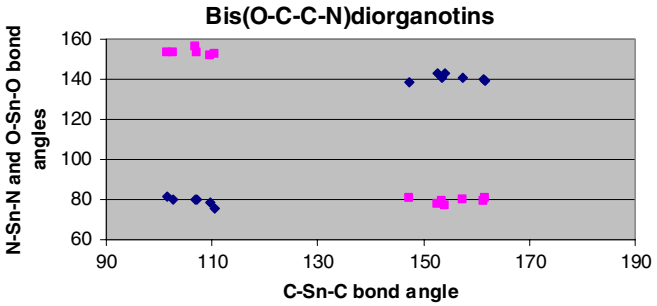

Fig. 24. Diamond points describe N–Sn–N bond angles, square points O–Sn–O angles. Both curves should cross each other for compounds "frozen" near the transition state (110° ⩽ C–Sn–C ⩽ 147°).

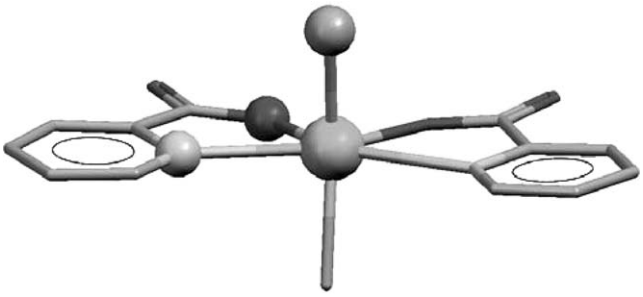

Fig. 25. X-ray structure of *trans*-di-*t*-butyl-bis(2-picolinato-*N*,*O*)-tin. Atoms that do not change position in the *trans–cis* pathway are shown as balls; all others as capped stick; *t*-butyl C atoms (except those bound to tin) and H atoms are omitted.

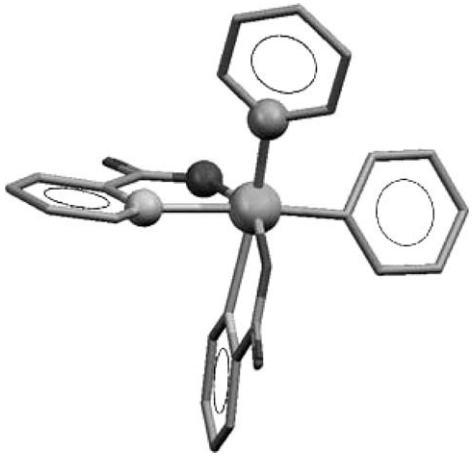

Fig. 26. X-ray structure of *cis*-diphenyl-bis(2-picolinato)-tin. Atoms that do not change position in the *trans–cis* pathway are shown as balls; all others as capped stick; H are omitted.

This model is further confirmed with a set of tetracyclo,O,O′ compounds (12 hits) having the chelating ligand shown in Scheme 2, X = any atom.

In the next plot, Fig. 28, O–Sn–O bond angles vs C–Sn–C bond angles display the same behavior as the picolinato derivatives above.

In the next plot, Fig. 29, curves of Sn–Op and Sn–Os bond lengths cross each other close to the transition state, in contrast with N,O ligands of Fig. 23 where Sn–O and

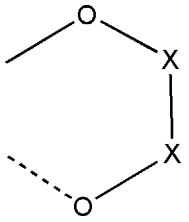

Scheme 2.

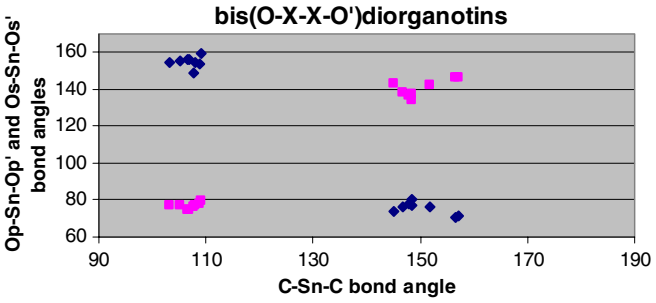

Fig. 28. Square points belong to Os–Sn–Os′ and diamond points to Op–Sn–Op′ angles. Both curves should cross each other for compounds "frozen" near the transition state (110° ⩽ C–Sn–C ⩽ 145°).

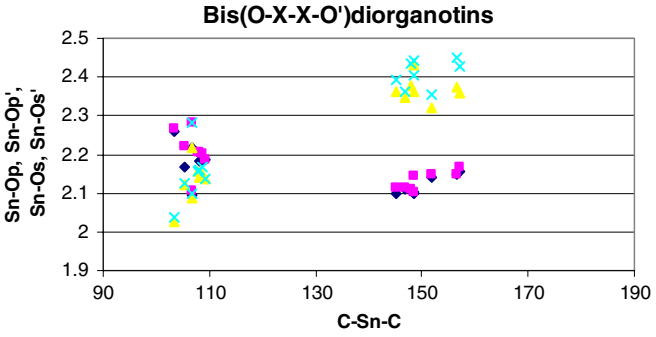

Fig. 29. *Trans*-like structures (147° ⩽ C–Sn–C ⩽ 160°) show Sn–Os and Sn–Os′ bond lengths (triangle and cross) located at the top of the plot; Sn–Op and Sn–Op′ ones (diamond and square) are at the bottom. The trend is opposite for *cis* structures (100° ⩽ C–Sn–C ⩽ 110°), suggesting that curves close to the transition state intercept.

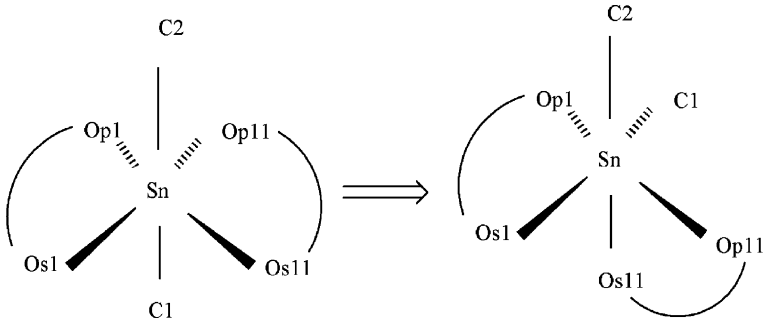

Fig. 27. *Trans* and *cis* form in the interconversion pathway.

Sn–N do not intercept. The affinity of Sn for O donors is stronger than for N donors and is responsible for the different behavior. Also, in the *cis* structures the Os atoms are now opposite to C atoms and form Sn–O bonds shorter than Sn–Op which are now *trans* to each other, see triangle and cross points for C–Sn–C lower than 115°.

From this set we see that *trans*-dimethyl-bis(3-hydroxy-2-methyl-4H-pyran-4-onato)-tin(IV) (refcode YIBWUB) [26] and *cis*-diphenyl-bis(3-hydroxy-2-methyl-4H-pyran-4-onato)-tin(IV) (refcode YIBXAI) [26] X-ray structures confirm the trend shown by *trans*-di-*t*-butyl-bis(2-picolinato-*N*,*O*)-tin (YORLIA) and *cis*-diphenyl-bis(2-picolinato)-tin (HATKOC), that is, in the *trans* to *cis* pathway Os and Os′ end up *cis* to each other whereas Op and Op′ end up *trans* to each other (Figs. 30–33).

Tin can increase its coordination sphere from 6 to 7 and 8 suggesting that solvent influence, very important in the *cis–trans* determination of many octahedral transition compounds but hard to detect in their crystal structures, can be visualized in its crystalline compounds. Aqua-dicyclohexyl-bis(2-picolinato)-tin(IV) ethanol solvate (refcode ERERUO) [27] and aqua-di-*n*-butyl-bis(2-pyridinecarboxylato-*N*,*O*)-tin (refcode EMOBOX) [28] show an additional molecule of water coordinated to tin in bipyramidal pentagonal polyhedra. Space for the incoming water molecule is provided by the large Qs–Qs′ area; this suggests further elements to evaluate factors influencing the *cis–trans* interconversion pathway.

Next, the molecule of aqua-di-*n*-butyl-bis(2-pyridinecarboxylato-*N*,*O*)-tin is shown.

Other factors influencing the coordination sphere shown in crystals are due to neighboring molecules. Thus, bis(*N*-acetylhydroxylamino)dimethyltin(IV) crystallizes as the *cis* form (C–Sn–C bond angle 109.1(4)°) [15] whereas the

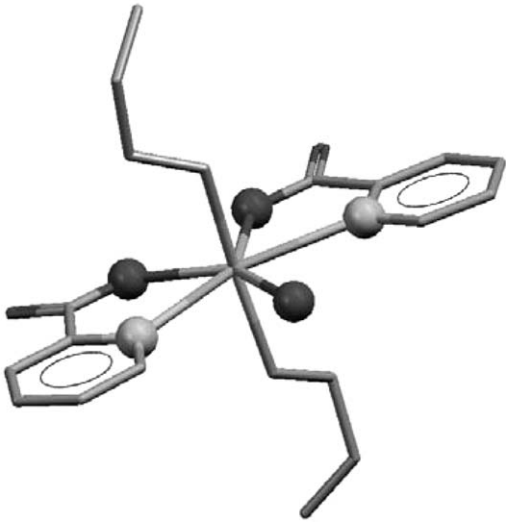

Fig. 32. X-ray molecular structure of aqua-di-*n*-butyl-bis(2-pyridinecarboxylato-*N*,*O*)-tin [28] showing its 7-coordinate bipyramidal pentagonal coordination sphere, the 5 atoms bound to tin the equatorial plane are depicted as balls, H atoms omitted.

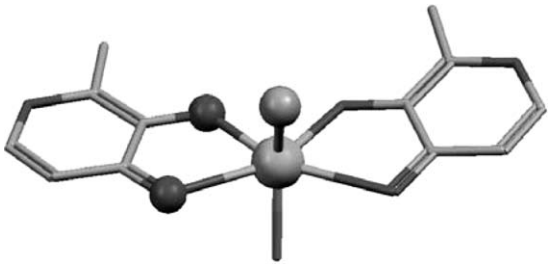

Fig. 30. X-ray structure of *trans*-dimethyl-bis(3-hydroxy-2-methyl-4H-pyran-4-onato)-tin(IV) [26]. Atoms that do not change position in the *trans–cis* pathway are shown as balls; all others as capped stick; H atoms are omitted.

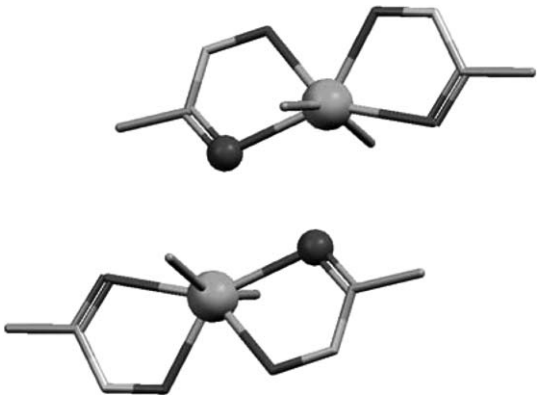

Fig. 33. X-ray molecular structure of *trans*-bis(*N*-acetylhydroxylamino)dimethyltin(IV), a dimer arrangement showing its distorted 7-coordinate bipyramidal pentagonal coordination sphere; the additional O atom, depicted as a ball, forms a weak Sn–O bond (2.98 Å).

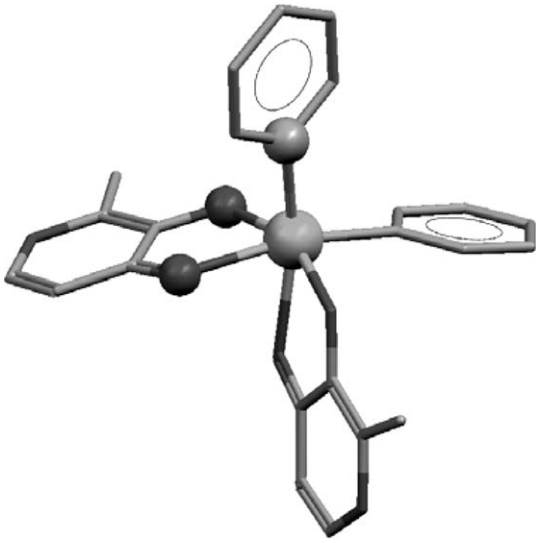

Fig. 31. X-ray structure of *cis*-diphenyl-bis(3-hydroxy-2-methyl-4H-pyran-4-onato)-tin(IV) [26]. Atoms that do not change position in the *trans–cis* pathway are shown as balls; all others as capped stick; H atoms are omitted.

trans form (C–Sn–C bond angle = 156.7(7)°) crystallizes as a hydrate, bis(*N*-acetylhydroxylamino)dimethyltin(IV) · H_2O [15], that has an additional Sn···O bond length of 2.98 Å and therefore is a dimer, shown below. Again the same Qs–Qs′ large space that was approached by an incoming water molecule to yield aqua-dicyclohexyl-bis(2-picolinato)-tin(IV) described above, is used; the distortion due to the 2nd unit (C–Sn–C bond angle equal 157.1°) is less than that of aqua-dicyclohexyl-bis(2-picolinato)-tin(IV) (C–Sn–C bond angle equal 180°).

Last, some anomalous structural features that appear for this *trans–cis* conversion pathway as shown in Figs. 4, 5 and 22, are due to one compound, *trans*-dimethyl-bis(1-phenyl-3-methyl-4-trichloroacetyl-5-pyrazolonato)- tin(IV) (refcode LIWKUX) [18]. This analysis suggests to us that results may be not accurate and that we need to reinvestigate its structure by recollecting crystal data.

3. Conclusions

We provide structural trends related to the octahedral *trans–cis* isomerization by using data stored in the CSD. These indicate good general agreement with the STB model for initial changes in C–Sn–C bond angles from the *trans* configuration towards the *cis* one. The number of chelate atoms induces different ranges of experimentally found STB structures. Thus, 6-membered O,O′ rings show configurations closer to 180° than 5-membered ones and so on: that is, greater octahedral deformation is associated with fewer number of chelating atoms. Trends observed in this paper depend also on the type of donor, that is S and O atoms have different covalent radii and so their chelates can be accommodated accordingly on the coordination sphere, e.g., the planarity of the S chelator may be more flexible.

The proposed model for this *trans–cis* interconversion pathway is associated with decreasing C–Sn–C bond angles and shows 2 weakly bound Q chelating donors lengthening their Sn–Q bonds, until the transition state (TS) is reached, and later strengthening when the *cis* isomer forms: they end up *cis* to each other. On the contrary, the 2 strongly bound donors are more involved in bonding to the metal until the TS is reached, and later less: they end up *trans* to each other. The entire process occurs through counter clockwise rotation of 3 bonds illustrated in Fig. 27.

The *trans–cis* isomerization process may be influenced by neighboring molecules, or solvent, interacting with tin at the Qs···Qs′ area; this implies a temporary increase of tin coordination number.

In this nondissociative Sn-donor bond process the TS needs to be further explored. The *trans* compound closest to the *cis* configuration, bis(chloroacetato)-(hexamethylene)-tin [29] (refcode LEDLAH), is a 7-membered cyclic diorganotin that stabilizes a C–Sn–C bond angle of 122°. Therefore fewer than 6 C atoms may be needed to make smaller C–Sn–C bond angles and permit visualization of the transition state closely. In addition, several donors in the chelate rings should be tested experimentally.

Acknowledgements

Christine Phillips, Ryan Meyer and Cristian Opazo for help with software, Vassar College Research Committee.

References

[1] J.C. Bailar, J. Inorg. Nucl. Chem. 8 (1958) 165.
[2] C.S. Springer, R.E. Sievers, Inorg. Chem. 6 (1967) 852.
[3] R.F. Zahrobsky, J. Coord. Chem. 1 (1971) 301.
[4] D.S. Dyer, R.O. Ragsdale, Inorg. Chem. 8 (1969) 1116.
[5] E. Turin, R.M. Nielson, A.E. Merbach, Inorg. Chim. Acta 134 (1987) 67.
[6] R. Kuroda, S. Neidle, I.M. Ismail, P.J. Sadler, Inorg. Chem. 22 (1983) 3620.
[7] R.C. Johnson, C.G. Wirmer, Inorg. Chem. 18 (1979) 2027.
[8] D. Donnecke, W. Imhof, J. Chem. Soc., Dalton Trans. (2003) 2737.
[9] I.A. Guzzei, C.H. Winter, Inorg. Chem. 36 (1997) 4415.
[10] E. Alessio, A. Sessanta, P. Faleschini, M. Calligaris, G. Mestroni, J. Chem. Soc., Dalton Trans. (1994) 1849.
[11] V.G. Kumar Das, Y.C. Keong, C. Wei, P.J. Smith, T.C.W. Mak, J. Chem. Soc., Dalton Trans. (1987) 129.
[12] K. Jurkschat, N. Pieper, S. Seemeyer, M. Schuermann, M. Biesemans, I. Verbruggen, R. Willem, Organometallics 20 (2001) 868.
[13] V.G. Kumar Das, Y. Chee-Keong, P.J. Smith, J. Organomet. Chem. 327 (1987) 129.
[14] B.N. Biddle, J.S. Gray, A.J. Crowe, J. Chem. Soc., Dalton Trans (1990) 419.
[15] P.G. Harrison, T.J. King, R.C. Phillips, J. Chem. Soc., Dalton Trans. (1976) 2317.
[16] D.L. Kepert, Progr. Inorg. Chem. 23 (1977) 1.
[17] P.G. Harrison, T.J. King, J.A. Richards, J. Chem. Soc., Dalton Trans. (1975) 826.
[18] F. Marchetti, C. Pettinari, M. Rossi, F. Caruso, Main Group Met. Chem. 21 (1998) 255.
[19] C. Sreelatha, D.K. Srivastava, V.D. Gupta, H. Noth, J. Chem. Soc., Dalton Trans. (1988) 407.
[20] P. Perez-Lourido, J. Romero, J.A. Garcia-Vazquez, A. Sousa, J. Zubieta, U. Russo, J. Organomet. Chem. 595 (2000) 59.
[21] C. Camacho-Camacho, R. Contreras, H. Noth, M. Bechmann, A. Sebald, W. Milius, B. Wrackmeyer, Magn. Reson. Chem. 40 (2002) 31.
[22] V.S. Petrosyan, N.S. Yashina, T.V. Sizova, T.V. Leonova, L.A. Aslanov, A.V. Yatsenko, L. Pellerito, Appl. Organomet. Chem. 8 (1994) 11.
[23] M. Gielen, A. Bouhdid, E.R.T. Tiekink, Main Group Met. Chem. 18 (1995) 199.
[24] K. Jurkschat, E.R.T. Tiekink, Main Group Met. Chem. 17 (1994) 659.
[25] M. Gielen, M. Boualam, E.R.T. Tiekink, Main Group Met. Chem. 16 (1993) 251.
[26] S. Bhattacharya, N. Seth, V.D. Gupta, H. Noth, K. Polborn, M. Thomann, H. Schwenk, Chem. Ber. 127 (1994) 1895.
[27] D. Dakternieks, A. Duthie, D.R. Smyth, C.P.D. Stapleton, E.R.T. Tiekink, Appl. Organomet. Chem. 18 (2004) 53.
[28] H.-D. Yin, C.-H. Wang, C.-L. Ma, Y. Wang, Chin. J. Chem. 20 (2002) 1608.
[29] X. Kong, T.B. Grindley, P.K. Bakshi, T.S. Cameron, Organometallics 12 (1993) 4881.